

# Indicators of convection derived from a bulk explicit microphysics scheme

Richard A. Dare

Bureau of Meteorology Research Centre, Australia

(Manuscript received May 2003; revised June 2004)

**Following theoretical developments over recent decades and improvements in computational resources, reasonably detailed representations of microphysics have been implemented into numerical weather prediction models at many operational forecasting centres. While the primary purpose of this work has been to improve the performance of the numerical models, microphysics schemes offer the potential to derive fields that may be of use to forecasters beyond the prediction of precipitation. Based on properties characterising aspects of convective activity, such as heavy precipitation, presence of hail, vertically deep clouds and lightning, four fields are defined that may be derived from a microphysics scheme. The four fields function as indicators of convective activity, based on explicitly modelled features. The states of the four convective fields are analysed at every model timestep and are then expressed as percentage occurrences in two-dimensional map form. These methods ensure that any simulation of convection is not overlooked and that forecasters receive information in a form that may be perused with ease. The production of the four indicators of convection during simulations of precipitation events of varying intensities demonstrates the potential use of the indicators as forecasting tools.**

## Introduction

There has been much progress in mathematical representation of microphysical processes in atmospheric models, including, for example, work by Marshall and Palmer (1948), Bigg (1953), Kessler (1969) and Wisner et al. (1972). Fortunately, developments in computing have been sufficient to allow development, implementation and execution of microphysical models based on the work of these, and other, authors. Operating at very high spatial resolutions, such models were used to produce simulations of cloud and hydrometeor evolutions, as presented by Orville and Kopp (1977), Hsieh et al. (1980) and Lin et al. (1983). Despite these advances, detailed models were not

used in operational forecasting due mainly to the inherent time constraints of such environments. However, in recent years, computational resources have reached a level that allows some inclusion of parametrisation of ice-phase particles in the microphysics component of operational models (Hong et al. 1998; Wilson and Ballard 1999; Bélair et al. 2000). In an operational environment, it is required, of course, that the microphysics scheme functions as an efficient component of the numerical model, producing an appropriate representation of moist processes (evolution of moisture distributions and latent heating) and an estimate of surface precipitation. Time constraints of this streamlined system prevent the depth of analysis that is possible during case studies, such as those discussed by Rutledge and Hobbs (1983). Further, while Rutledge and Hobbs

---

*Corresponding author address:* R. Dare, Bureau of Meteorology Research Centre, GPO Box 1289K, Melbourne, Vic. 3001, Australia.  
Email: r.dare@bom.gov.au

studied the evolution of specific systems within a relatively small two-dimensional domain, the range of systems that may develop throughout larger and three-dimensional grids means that even given time, the task of analysing the evolution of hydrometeors must be even more involved and time consuming. While not aiming to analyse numerical results in the same manner as Rutledge and Hobbs, it is proposed that further use may be made of a microphysics scheme, even when functioning in an operational model. Moisture fields and microphysical terms are, of course, available within microphysics schemes, but are generally not examined in detail. Analysis of these data in an automated manner may be useful in extracting information concerning development of weather systems.

The present work involves development of four fields derived from a microphysics scheme, with the aim of providing guidance in regard to prediction of convective precipitation events. Here, the terms convection, convective precipitation and convective activity refer to the general development of vertical motions in the atmosphere that form cumulus clouds and produce precipitation that is typically of greater intensity than those produced by frontal or orographic influences. Horizontal spatial scales of convective cells and systems containing cells increase upwards from about 10 km to include systems such as squall lines and supercells. To be suitable for execution within an operational environment, the derived fields must be computed efficiently and finally available in a ready and concise format for easy perusal by, for example, forecasters.

As it has been recognised that the prediction of severe weather is a serious challenge, other methods for the prediction of convective activity based on numerical model output have been developed in the past. Such schemes include the Mills and Colquhoun (1998) severe thunderstorm decision tree and the Hanstrum et al. (2002) cool-season tornadic thunderstorm potential diagnostic. Compared with the present work, these schemes contain quite sophisticated methods of predicting, and differentiating between types of, convective activity. The present work differs from these diagnostics by its inclusion and consideration of a microphysics scheme and its evaluation of explicitly modelled distributions of hydrometeors at every model time step.

Some details of the microphysics scheme and the model used are given in the next section. This is followed by a discussion of the definitions of the four fields to be used as indicators of convection. Examples of the fields produced and comparison with observations during a number of precipitation events are shown next. Summary and conclusions are made in the final section.

## The bulk explicit microphysics (BEM) scheme

The bulk explicit microphysics scheme developed at the Bureau of Meteorology Research Centre defines equations controlling the evolutions of six classes of water (water vapour, cloud water, rain water, cloud ice, snow and hail/graupel). The label 'bulk' refers to the gross representation of individual hydrometeor classes, where each is generally represented at each point within the three-dimensional model grid by a mixing ratio alone, with size distribution of precipitating classes assumed to follow the Marshall and Palmer (1948) relationship. This differs from the more detailed bin microphysical schemes (Hall 1980) in which variables for specific hydrometeor size intervals are predicted; such schemes are computationally expensive and are currently unsuitable for operational modelling. The term 'explicit' refers to the property of the scheme to represent individual microphysical processes that are believed to occur in the atmosphere, rather than, for example, a single parametrisation approximating a series of processes. Examples of individual processes defined by the BEM scheme are condensation of water vapour to form cloud water, autoconversion of cloud water to form rain water, the gravity-driven fall of rain water and evaporation of rain water, which increases the local mixing ratio of water vapour. The BEM scheme is based on a large number of sources, including Byers (1965), Kessler (1969), Wisner et al. (1972), Lin et al. (1983), Rotstain (1997) and Lopez (2002). Details of the scheme's formulation and implementation are documented by Dare (2004).

The BEM scheme is operated within the framework of the LAPS model (Puri et al. 1998). In the present work, the horizontal grid resolution is  $0.050^\circ$  (grid spacing approximately 5 km). The particular domain used, corresponding to an operational domain used during recent years, covers the State of Victoria and Bass Strait in southeastern Australia (Fig. 1), with grid dimensions of 190 x 140 and 29 levels. Lateral boundary updates are provided by the Australian region  $0.375^\circ$  LAPS model. A convection parametrisation is not activated for experiments presented here, with the BEM scheme defining both stratiform and convective clouds. Although there are both positive and negative arguments surrounding the deactivation of a convection scheme in a model with grid spacings around 5 km (Molinari and Dudek 1992; Kuo et al. 1997), discussion of this issue is beyond the scope of the present work. Regardless of the conclusions of such a discussion, the chosen configuration of moist processes used here does in fact provide a suitable basis for an examination of the indicators of convection, the subject of this work.

**Fig. 1** Locations of the model domain (MD) and the sub-domain (SD) area of interest, centred approximately on Port Philip Bay and the city of Melbourne in Victoria, southeastern Australia.



## Indicators derived from the BEM scheme

To extract information that may be indicative of convection from a microphysics scheme, characteristics of convective activity in the atmosphere must be identified. These characteristics must be expressible in forms consistent with those of the microphysical fields. They should also be simple enough to assess efficiently while still providing useful information. Characteristics of convection considered here include moderate to large rates of precipitation, presence of hail, deep vertical columns of condensed or frozen water and lightning. There are, of course, many other characteristics that might be considered but these four are quite adequate for the present demonstration. Note that these characteristics are based purely on microphysical parameters. While other definitions, such as those involving temperature profiles or wind fields (Mills and Colquhoun 1998; Hanstrum et al. 2002), may also be used, or in future combined with those discussed in this section, the aim of the present work is to base the indicators on the explicitly modelled fields generated by the microphysics scheme. This means that the indicators function in a prognostic manner, while other schemes, though more complex (Hanstrum et al. 2002) are diagnosed from the model forecast environment.

### Format of convective indicators

It is important to minimise any increases in the computational resources required by the numerical model

due to the inclusion of the indicators. Of equal importance is the consideration of the presentation of numerically generated information. It might seem convenient to base the indicators on analyses of the state of the model-generated fields at the frequency of output of standard model fields, which might be one, three or six-hourly. However, this practice would avoid consideration of events that occur within these time intervals. This problem is exacerbated by the fact that the subject of interest is convective weather, in which life cycles are often of short duration. The approach used here, outlined as follows, is designed to overcome these problems. The highest temporal resolution possible and the most basic time-scale defined by the model is the timestep. More specifically, the physics timestep used currently in LAPS 0.050° is four minutes. A simple way to record and present information at this resolution, while avoiding flooding the forecaster with information, is to express events occurring over a single timestep as a percentage of a longer period, say three hours. This allows multiple occurrences of a specific event to be recorded in a single field rather than either using numerous fields to cover the three-hour period or neglecting weather that occurs within this period.

The indicator fields represent the atmospheric column over each horizontal grid-point. To store the fields of indicators in an efficient manner, the characteristics of the atmosphere are essentially extracted from the model's three-dimensional fields and placed onto a two-dimensional map. Following definition of supposed relevant structures (distributions of hydrometeors and associated tendencies) within a column, each column of the model atmosphere is examined individually during determination of convective properties. When the conditions within a column satisfy the definition, the particular indicator is said to be activated, and the corresponding point on the two-dimensional grid is incremented by a value proportional to the fraction of the model timestep divided by the (three-hour) time period between output of model fields. The addition of just four two-dimensional fields is not expected to significantly over-burden available resources, as the bulk of the model-generated data consists of substantially larger three-dimensional fields.

### Definitions of convective indicators

The definitions of the four convective indicators are discussed in this section. Indicators are numbered, named and described briefly in Table 1.

The method of identifying convective precipitation based on its intensity has been used by Churchill and Houze (1984), Steiner and Waldvogel (1987), Johnson and Hamilton (1988) and Yuter and Houze

**Table 1. Definitions of indicators of convection.**

<i>Indicator number</i>	<i>Name of indicator</i>	<i>Definition of indicator</i>
1	Large rate of precipitation	Precipitation detected above a threshold rate
2	Hail potential	Hail/graupel mixing ratio above a threshold value at certain levels above the ground
3	Hydrometeor column	Deep column of liquid or frozen hydrometeors
4	Lightning	Separation of (implied) charge by falling hail/graupel

(1997). Indicator number 1, the large rate of precipitation, uses the same basic method. The rate at which precipitation is reaching the ground is compared with a specified threshold rate ( $5 \text{ mm h}^{-1}$ ). When the threshold is exceeded, the indicator is activated. Of course, this simple method does not consider the state of the atmosphere and on its own does not provide a robust guide to the presence of convective activity. To varying extents, all of the indicators of convection have this problem. This can be partly overcome by examining the activation of multiple indicators over the same period, with greater consistency among indicators increasing confidence. However, it should be remembered that the indicators are dependent on the performance of the model and in particular on the microphysics scheme, which ultimately depend on the accuracy of the initial condition.

The presence of hail is a useful indicator of convection. The second indicator is activated by the presence of a hail/graupel mixing ratio above a threshold value ( $5.0 \times 10^{-4} \text{ kg kg}^{-1}$ ) anywhere within a chosen layer of the atmosphere (from the ground up to  $\sigma$ -level = 0.6, where the  $\sigma$ -level is pressure divided by surface pressure). Although the potential for hail to reach the surface depends additionally on the temperature and moisture characteristics of the atmosphere between the ground and the location of the hail/graupel, this definition of convective activity is expected to provide a reasonably useful indication of convective activity while its simplicity ensures computational efficiency.

Identification of a relatively deep and vertically-continuous column of liquid or frozen hydrometeors indicates the presence of a cloud that is more likely to belong to the cumuliform rather than stratiform class. Activation of indicator number 3 requires that the total mixing ratios of all liquid and ice hydrometeors at every model level from the ground to  $\sigma$ -level = 0.6 exceed a threshold value ( $6.0 \times 10^{-6} \text{ kg kg}^{-1}$ ).

Determination of the fourth indicator (lightning) depends on a method of implying the existence of charge and charge separation based on microphysical terms. Models of electrification and lightning, such as

those used by Ziegler et al. (1991), Schuur and Rutledge (2000b) and Sun et al. (2002), are not utilised in the present work. The basis of the method is the belief that generation of charge results from collisions between hail/graupel and ice crystals followed by separation of charge due to differing rates of sedimentation (Gilmore and Wicker 2002). This is expressed in a relatively simple manner in terms of properties of the microphysics scheme as follows. Activation of the indicator requires the presence of a significant amount of cloud ice and snow ( $> 5.0 \times 10^{-4} \text{ kg kg}^{-1}$ ) within a specified vertical distance (two model levels) from where the rate of gravity-driven fallout of hail/graupel exceeds some threshold ( $2.8 \times 10^{-10} \text{ kg kg}^{-1} \text{ s}^{-1}$ ). Explicit mechanisms of charging, states of polarity and influences of temperature are not considered here. Other experiments (not discussed in the present work) have shown that supercooled liquid water may also be a useful parameter to consider in defining the lightning indicator. This is consistent with the work of Saunders et al. (1991), Schuur and Rutledge (2000a), Gilmore and Wicker (2002) and Atlas and Williams (2003). Note that the accuracy of this lightning field has not yet been assessed using observations of lightning; while this is a future task, the field produced here represents one component in a set of convective indicators.

## Results: assessment of convective indicators

The performance of the convective indicators is examined by comparing them with observations. The four fields are generated during numerical simulations of two separate 24-hour periods, each containing precipitation events over central Victoria. Figure 1 illustrates the location of the model domain over southeastern Australia, and the smaller sub-domain within it, centred approximately on Port Phillip Bay, over which the indicators were evaluated. For this initial assessment of the accuracy of the indicators, radar observations are used as a guide to the presence of convection, based on rain rates, spatial distribu-

tions and temporal evolution of precipitating systems. Yuter and Houze (1997) note that both intensity and texture of the precipitation may be used to identify convective regions. Surface observations are used to verify the interpretation of the radar observations. For the small number of cases considered here, the use of these subjective methods for differentiating convective and stratiform rainfall is quite adequate, particularly considering the difficulties in objective differentiation, as shown by the discussions of Tokay and Short (1996), for example. Discussions presented by Yuter and Houze (1997) demonstrate that objective methods are naturally derived from reasoned subjective observations and conclusions. Although the convective indicators are compared with radar observations, note that it is not the aim to predict radar reflectivities. Advantages of the production of the present indicators of convection over radar reflectivities are that the indicators account for a variety of convective features, rather than a reflectivity that is primarily proportional to mixing ratio, and they also consider events over a period of time rather than an instantaneous field.

As noted earlier, the fields of convective indicators are expressed as percentages on two-dimensional maps. There are several ways in which these may be interpreted. One should not necessarily interpret the percentage as a probability of that convective property occurring at the location indicated. As each convective indicator is computed based on its occurrence in the model's atmosphere, activation of an indicator, with a value of say 10 per cent, could be interpreted to mean that a convective feature may occur and be relatively short-lived. A larger value, such as 80 per cent, might mean that there is some chance of development of the feature and if it does develop, it may have a significant lifetime. Alternatively, one could interpret it to mean that the feature is very likely to develop. One might choose to further use the percentage to estimate the lifetime or intensity of the convection. The performances of the model in general and of the microphysics scheme in particular also affect the percentage values produced by an indicator. The values of parameters used to determine thresholds are a further influence. Although one might find some use in the interpretation of the percentages attached to the convective indicators, using the indicators as a guide to the general location and timing of convection is a simple and apparently useful method, as demonstrated by the following examples. Note that while these examples involve discussion of observed events, the aim is to demonstrate the operation of the convective indicators rather than to discuss the actual events in detail.

### Precipitation events on 14 June 2002

During the 24-hour period 0000 UTC 14 June 2002 to 0000 UTC 15 June 2002, a trough approached the area of interest from the southwest (Fig. 2). Associated with this was a small drop in pressure over western and central Victoria, while the surface winds remained close to northwesterly. Two main episodes of precipitation occurred over central Victoria under the influence of these conditions. The first of these, occurring from 0000 to 1200 UTC, exhibited light, scattered rainfall, that was interpreted as non-convective (Fig. 3). The second event involved development of significant precipitation to the north of Melbourne from 1400 UTC onwards (Fig. 4). This was followed by further development and movement to the southeast (Fig. 5) and dissipation by about 2200 UTC. Compared with the first episode, the rainfall intensity was greater while the spatial extent of the system was relatively limited, allowing it to be classified as convective. The differences between these two relatively short-lived events serve as a simple test of the ability of the convective indicators to differentiate between convective and stratiform precipitation.

The prediction of convective activity for the period 0600-0900 UTC based on indicator number 3 alone is shown by Fig. 6. Note that indicator numbers 1, 2 and 4 did not trigger during the period 0600-0900 UTC and are therefore not shown. The fact that only one of the four was activated suggests that either there was little convection present or that indicator number 3 may be over-active. Comparing the relatively light precipitation observed (Fig. 3) with prediction (Fig. 6) confirms that indicator number 3 was over-active while numbers 1, 2 and 4 have reacted appropriately, avoiding generation of false alarms. Of course, the parameters used to define thresholds may be adjusted to reduce the over-activity exhibited by indicator number 3. Alternatively, it might be useful to allow a single indicator to produce such results to provide a guide to the presence of convection which may otherwise be missed by less sensitive indicators, while generally its results may be tempered, in one's mind, through the additional consideration of the other fields.

Between 1200 and 1500 UTC, all four indicators detect convection over central Victoria (Fig. 7). Again, indicator number 3 is the most active, but there is agreement between the four fields. The location of predicted convection compares reasonably well with that of the rainfall observed (Fig. 4). During the three-hour period that follows, the indicators predict an increase in the system's size and movement to the southeast (Fig. 8). Indicator number 4 (Fig. 8(d)) probably compares best with observations (Fig. 5). The agreement between these fields may suggest that the model-generated features are indeed convective.

Fig. 2(a) MSLP at 0000 UTC 14 June 2002 over south-eastern Victoria.

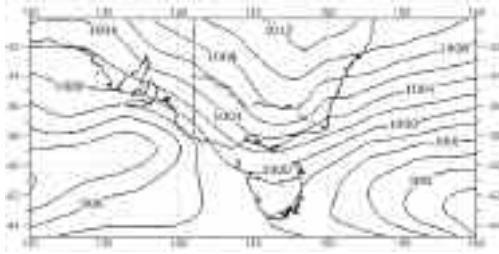


Fig. 2(b) MSLP at 1200 UTC 14 June 2002 over south-eastern Victoria.

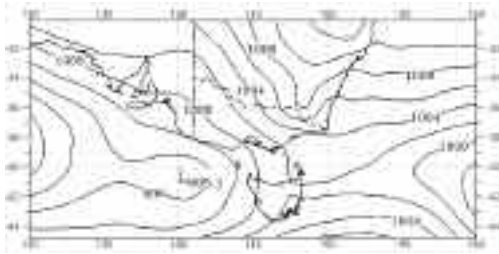
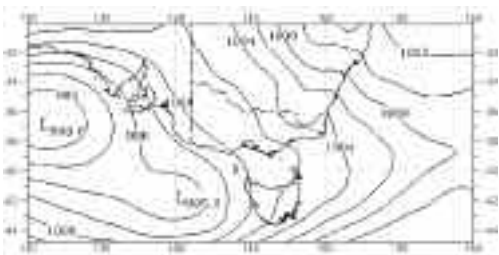


Fig. 2(c) MSLP at 0000 UTC 15 June 2002 over south-eastern Victoria.



Further, agreement between the fields may be interpreted to mean that reliability of indicator-based prediction of these features is increased, although more testing is required to support such a conclusion.

While the relationships between the convective indicators and the fields generated by the microphysics scheme were explained in an earlier section, it is worthwhile reviewing the functioning of these relationships at times during the model simulation. Figure 9 illustrates the presence of various classes of hydrometeor at 0300 UTC in a latitude-height cross-section to the west of Melbourne. Although the micro-

Fig. 3 Radar observed rainfall rates at 0700 UTC 14 June 2002.

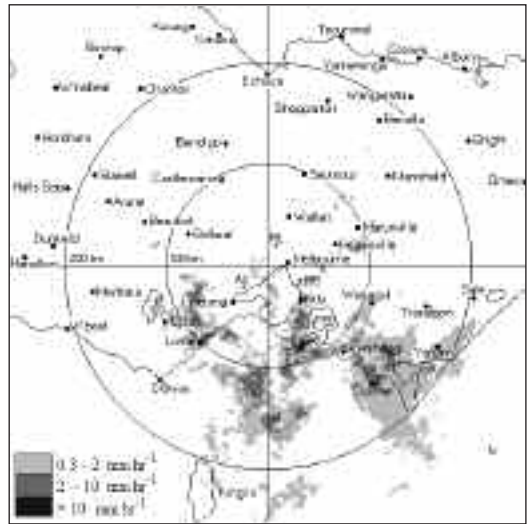
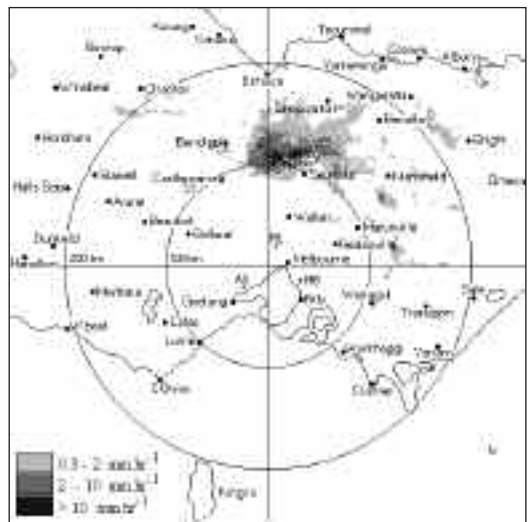


Fig. 4 Radar observed rainfall rates at 1500 UTC 14 June 2002.



physics scheme has generated a significant amount of cloud water and a spatially extensive distribution of ice-phase particles, the convective indicators were not activated in this example because the required conditions were not met. Note that the radar observations confirm the presence of only light rain at 0300 UTC, which is consistent with conclusions based on the numerical results.

It is interesting to examine fields produced by the microphysics scheme when the indicators of convection are triggered. A similar north-south oriented cross-section, this time located a short distance to the

**Fig. 5** Radar observed rainfall rates at 1900 UTC 14 June 2002.

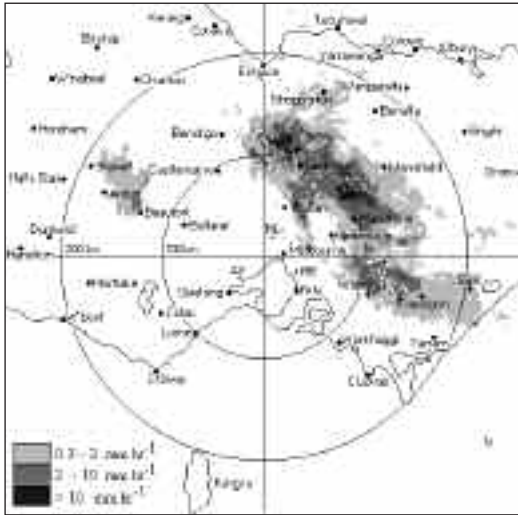
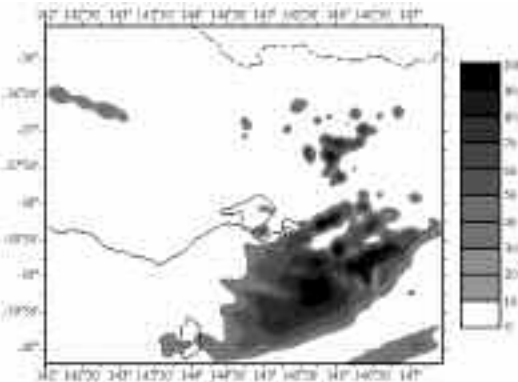


**Fig. 6** Convective indicator number 3 for the period 0600-0900 UTC on 14 June 2002. Shading is applied based on a contour interval of 10%.



east of Melbourne, again shows the presence of cloud water and ice-phase particles (Fig. 10). There are several cloud types simulated in this example; stratus from about 39° to 40°S with cloud base around 875 hPa, clouds that may be classified as stratocumulus (38° to 39°S) and a deep column of water near 37°S representing cumulus convection. Note the correspondence between the columns of hail and the columns of water and snow near 37° and 37°30'S. Such a convective situation is detected by the indicators based on several of the criteria presented earlier. In this example, the following properties may be detected: (1) the

**Fig. 7(a)** Convective indicator number 1 for the period 1200-1500 UTC on 14 June 2002. Shading is applied based on a contour interval of 10%.

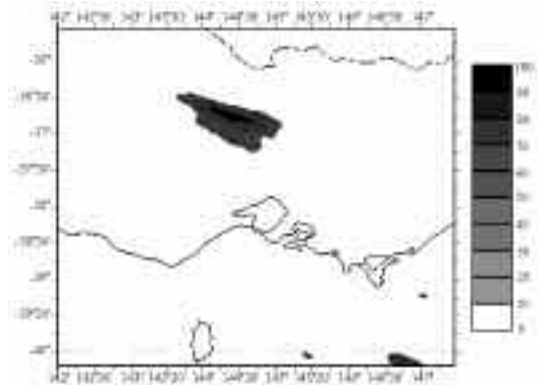


**Fig. 7(b)** Convective indicator number 2 for the period 1200-1500 UTC on 14 June 2002. Shading is applied based on a contour interval of 10%.

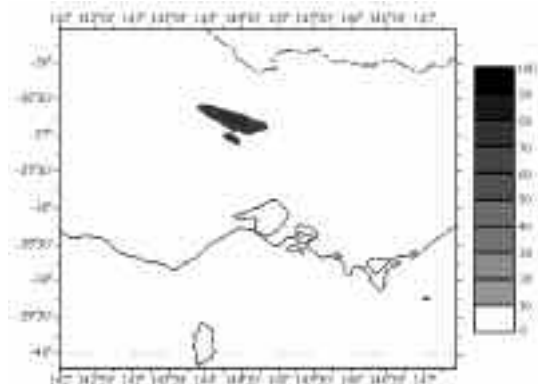


**Fig. 7(c)** Convective indicator number 3 for the period 1200-1500 UTC on 14 June 2002. Shading is applied based on a contour interval of 10%.

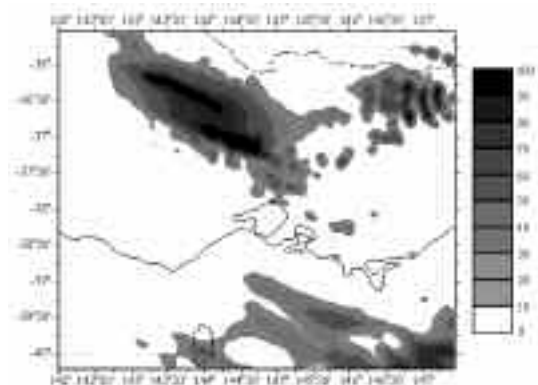
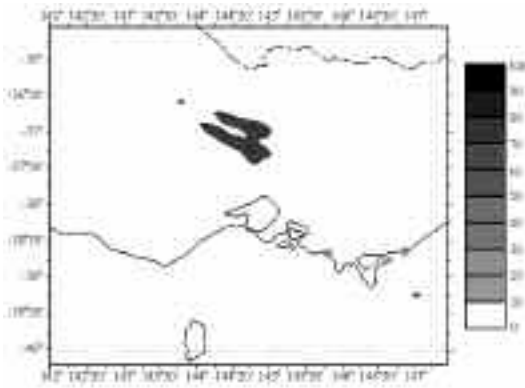


**Fig. 7(d) Convective indicator number 4 for the period 1200-1500 UTC on 14 June 2002. Shading is applied based on a contour interval of 10%.**



presence of the columns of hydrometeors; (2) the presence of a significant amount of hail near the 600 hPa level; and (3) a large rate of precipitation that results from the large cloud-water content a short distance above the surface near 37°S. Although this example is an instantaneous picture of the distribution of hydrometeors, there is good agreement with the three-hourly accumulated convective indicators shown in Fig. 8 at longitudes near 145°30'.

In summary, two separate precipitation events occurred during the 24-hour period. The most active indicator (number 3) identified both events. However, as required, the other three triggered for the second event only. Overall, these are positive results because the general locations and timings of the precipitation events were identified successfully by the indicators. Importantly, the different approaches used by the individual indicators proved effective. In making comparisons between the convective indicators and observations, one must remember that the indicators cover a period of three hours, while the observations consist of virtually instantaneous radar pictures. Also note that the aim here is not to simulate radar observations but to produce indications of convective activity based on fields produced by the microphysics scheme.

#### **Precipitation events on 2 August 2002**

In the previous example, observations were presented first, followed by comparison with the four convective indicators. While this approach allowed a reasonable examination of the performance of the indicators, it was essentially a diagnostic exercise and did not necessarily provide an accurate indica-

**Fig. 8(a) Convective indicator number 1 for the period 1500-1800 UTC on 14 June 2002. Shading is applied based on a contour interval of 10%.**

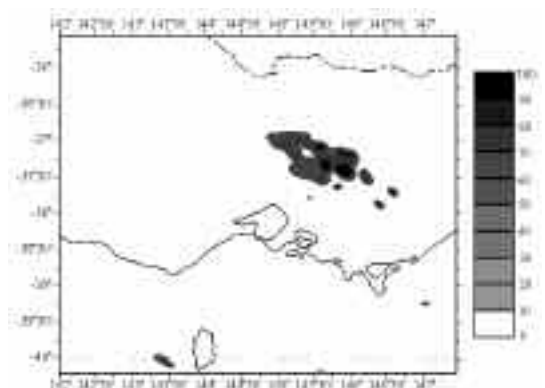


**Fig. 8(b) Convective indicator number 2 for the period 1500-1800 UTC on 14 June 2002. Shading is applied based on a contour interval of 10%.**

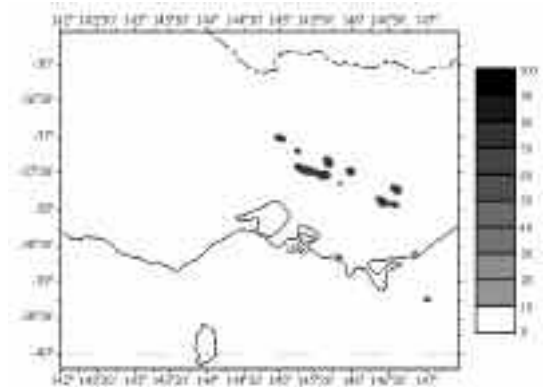


**Fig. 8(c) Convective indicator number 3 for the period 1500-1800 UTC on 14 June 2002. Shading is applied based on a contour interval of 10%.**

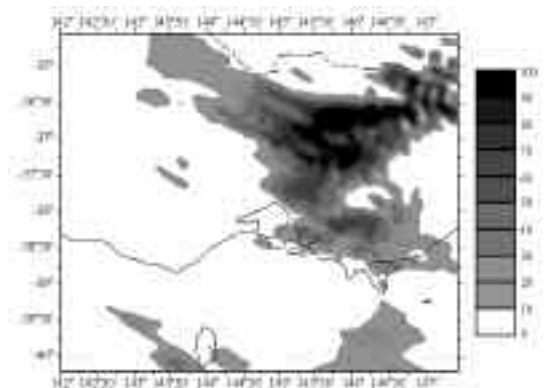
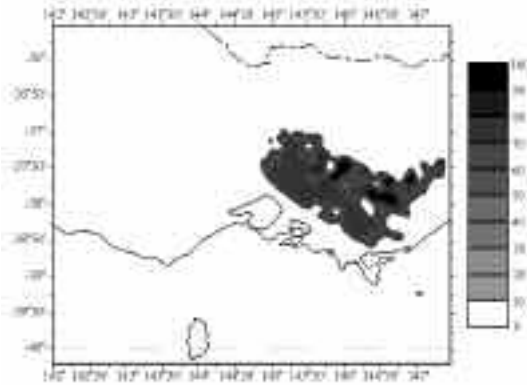


**Fig. 8(d)** Convective indicator number 4 for the period 1500-1800 UTC on 14 June 2002. Shading is applied based on a contour interval of 10%.



tion of the potential ability of the convective indicators to function as forecasting tools. The approach used in this second example is different. With the aim of following the general point of view of a forecaster, the convective indicators are presented and discussed first, then these are compared with observations of the atmosphere.

One might have expected convective activity over central Victoria as a trough approached from the west during the 24-hour period 0000 UTC 2 August 2002 to 0000 UTC 3 August 2002 (Fig. 11). Therefore, it may be useful to peruse information concerning prediction of convective activity, such as the maps of the four convective indicators. First, a time-series of the lightning indicator is examined (Fig. 12). Results covering the periods 0000-0300 and 0300-0600 UTC are not shown because no convective activity was predicted by this indicator. During the period 0600-0900 UTC, the indicator predicts convection on the coast at around 143°30'E (Fig. 12(a)). The northerly component of the flow results in movement of this feature to the south between about 0900 to 1500 UTC (Figs 12(b) and 12(c)). During the latter half of this period, there may also be development of smaller convective features over eastern Victoria. Figure 12(d) shows that there is a change in the convective situation during 1500-1800 UTC, with widespread development across the domain and movement of these convective features to the south. Note that these lines represent storm tracks over a period of three hours; they should not be interpreted as north-south oriented squall lines moving eastwards. Figures 12(e) and 12(f) next show

**Fig. 9** Latitude-height cross-section of mixing ratios of cloud water (colour shading), aggregates/snow (black contours) and hail/graupel (red contour) at longitude 144°30' at 0300 UTC 14 June 2002. The variable contour intervals cover mixing ratios ranging from  $2 \times 10^{-5}$  to  $5 \times 10^{-4}$  kg kg<sup>-1</sup>.

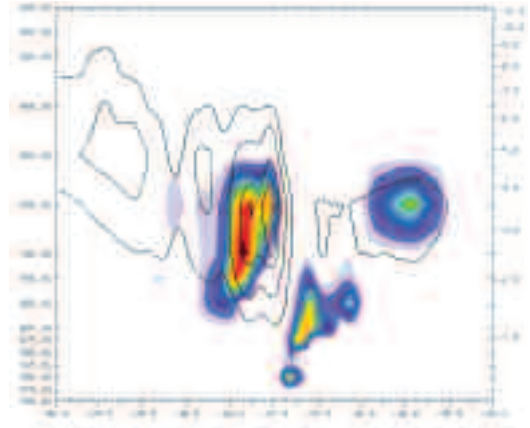
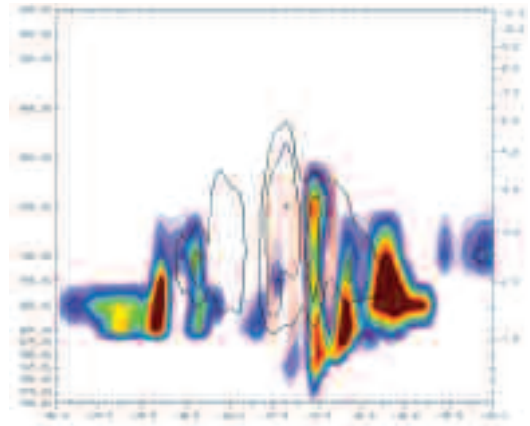


**Fig. 10** Latitude-height cross-section of mixing ratios of cloud water (colour shading), aggregates/snow (black contours) and hail/graupel (red contours) at longitude 145°30' at 1800 UTC 14 June 2002. The variable contour intervals cover mixing ratios ranging from  $2 \times 10^{-5}$  to  $5 \times 10^{-4}$  kg kg<sup>-1</sup>.



that these extensive developments of convection move further to the south and over the sea during the final six hours of the 24-hour period.

The predictions outlined above, based on indicator number 4, are supported by the other three indicators. To avoid presenting further predictions covering the

**Fig. 11(a)** MSLP at 0000 UTC 2 August 2002 over south-eastern Victoria.

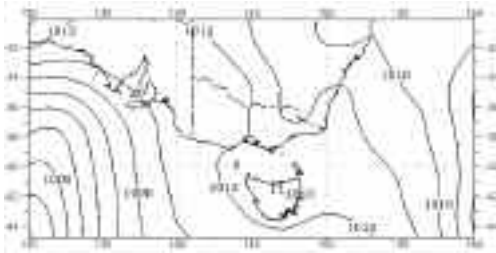


**Fig. 11(b)** MSLP at 1200 UTC 2 August 2002 over south-eastern Victoria.

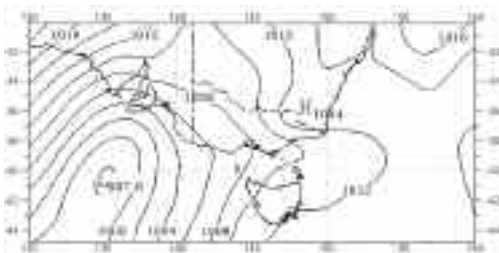
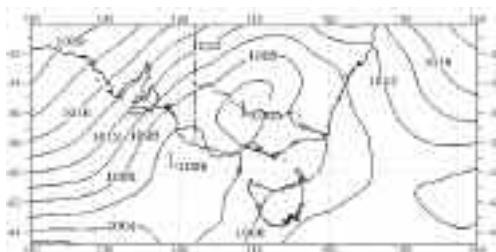


**Fig. 11(c)** MSLP at 0000 UTC 3 August 2002 over south-eastern Victoria.



entire 24-hour period, only one three-hour period map is shown for each of the three remaining indicators. The convective activity predicted over the coast during the period 0600-1200 UTC was also produced by indicator number 3, except that it also predicted some activity about three hours earlier (Fig. 13). The movement to the south was supported by indicator number 1 (Fig. 14). Development of widespread convection over the centre of the domain during 1500-1800 UTC

**Fig. 12(a)** Convective indicator number 4 for the period 0600-0900 UTC on 2 August 2002. Shading is applied based on a contour interval of 10%.

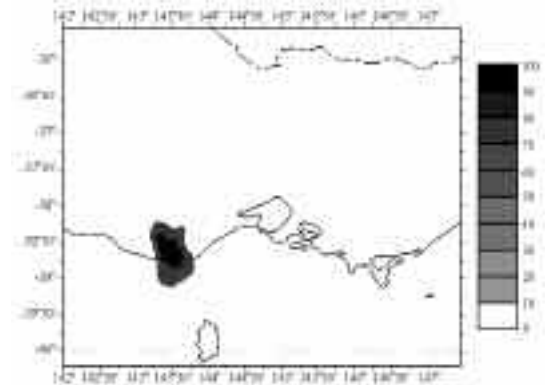


**Fig. 12(b)** Convective indicator number 4 for the period 0900-1200 UTC on 2 August 2002. Shading is applied based on a contour interval of 10%.

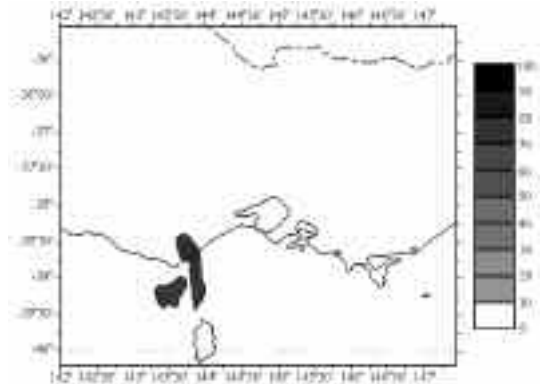


**Fig. 12(c)** Convective indicator number 4 for the period 1200-1500 UTC on 2 August 2002. Shading is applied based on a contour interval of 10%.

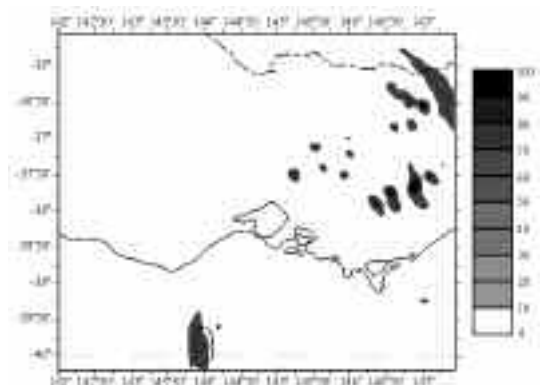


**Fig. 12(d)** Convective indicator number 4 for the period 1500-1800 UTC on 2 August 2002. Shading is applied based on a contour interval of 10%.

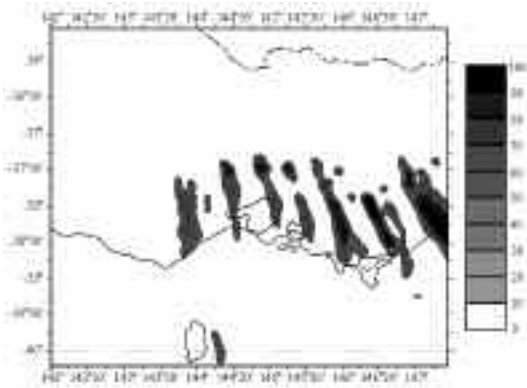


**Fig. 13** Convective indicator number 3 for the period 0300-0600 UTC 2 August 2002. Shading is applied based on a contour interval of 10%.

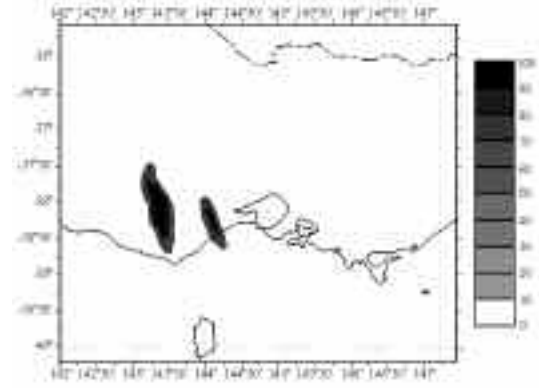


**Fig. 12(e)** Convective indicator number 4 for the period 1800-2100 UTC on 2 August 2002. Shading is applied based on a contour interval of 10%.

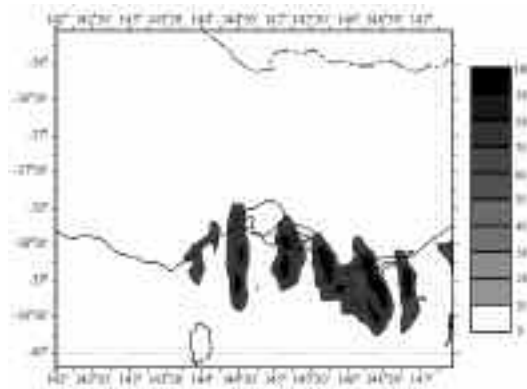


**Fig. 14** Convective indicator number 1 for the period 0900-1200 UTC 2 August 2002. Shading is applied based on a contour interval of 10%.

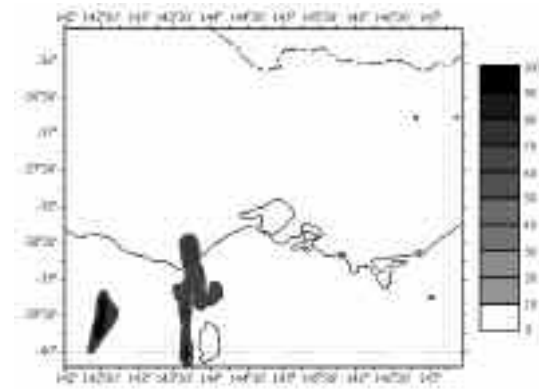


**Fig. 12(f)** Convective indicator number 4 for the period 2100 UTC 2 August to 0000 UTC 3 August 2002. Shading is applied based on a contour interval of 10%.

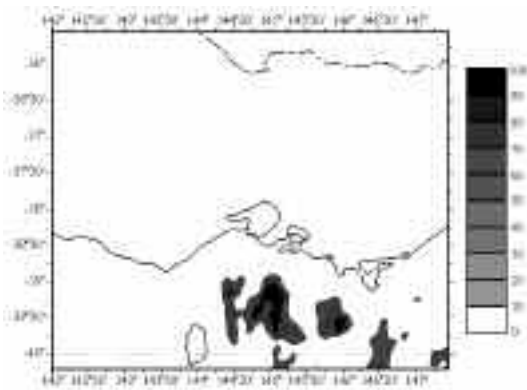
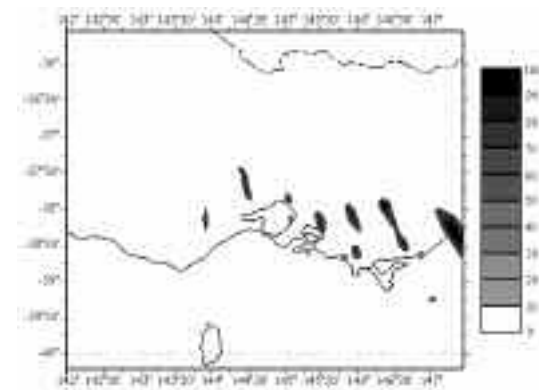


**Fig. 15** Convective indicator number 2 for the period 1500-1800 UTC 2 August 2002. Shading is applied based on a contour interval of 10%.



was predicted by indicator number 2 (Figure 15). Given the good agreement between the indicators, the forecast may be summarised as follows:

- From 0300 to 1500 UTC, development of convection is expected around the coastline between about 143°E and 144°E. This activity is expected to move out over the sea during this period. There may also be some smaller scale convection over the east of the State.
- After 1500 UTC, widespread convection may develop over central Victoria and move gradually to the south and off the coast by the end of the 24-hour period.

This forecast can now be compared with observations. From about 0000 to 0600 UTC, there were many small-scale, light to moderate-intensity areas of precipitation scattered over eastern Victoria. These were not predicted by the four indicators but this is a satisfactory result because these areas of precipitation did not appear to be convective. The first clear signs of convection appeared between 0600 and 1300 UTC, when small-scale areas of large intensity precipitation, apparently convective, developed approximately west and southwest of the bay. This is represented by the 0730 UTC radar image (Fig. 16). By 1130 UTC, the presence of convection is largely restricted to the inner western region of the domain (Fig. 17). Together, Figs 16 and 17 show the occurrence of convective activity from Ballarat to King Island. This means that the first point of the forecast above is reasonably accurate in terms of general location and timing. However, the second point of the forecast predicted convective development over different locations with quite different spatial extents. This can now be tested by comparing with observations.

After about 1700 UTC, the most significant convective activity discussed so far, in either 24-hour period, started to develop over central Victoria (Fig. 18). These patches developed into widespread and intense precipitation (Fig. 19), finally moving south towards the sea to complete this 24-hour period (Fig. 20). Probably the main problem with this second part of the forecast was that the model moved the convection southwards too soon. While the specific storm tracks produced by the model appear to be not identical to radar images, the convective activity was certainly identified in terms of both location and timing: compare Figs 12(d) and 12(e) with observations (Figs 19 and 20).

As found for the test based on the June event, the convective indicators have again performed well by providing useful guidance to the general locations and timings of the various developments of convective activity during this August event.

**Fig. 16** Radar observed rainfall rates at 0730 UTC 2 August 2002.

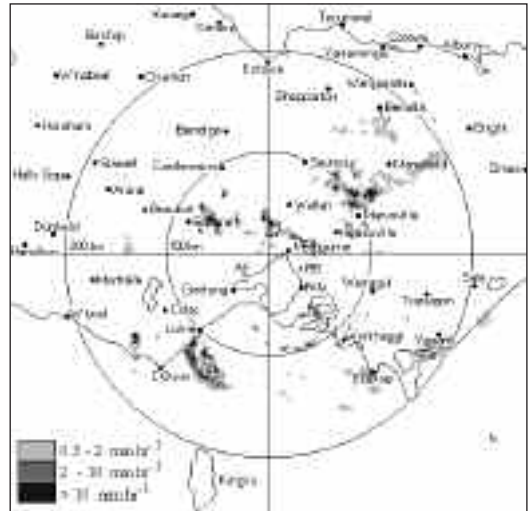
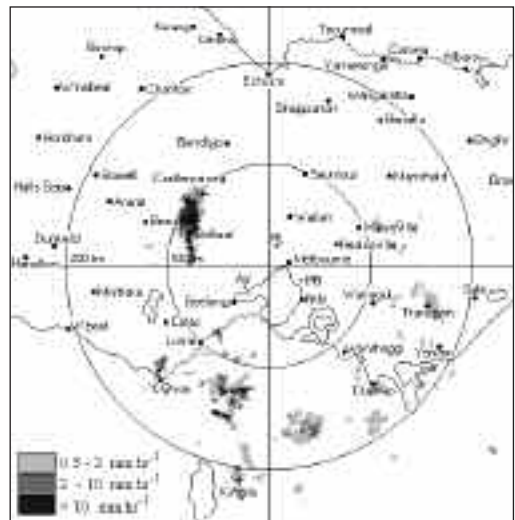


**Fig. 17** Radar observed rainfall rates at 1130 UTC 2 August 2002.



## Summary and conclusions

Traditionally, the fields available from a numerical weather prediction model were largely those involved in the model's basic dynamics and thermodynamics (winds, pressure, temperature and water vapour). Over recent years as the complexity of model physics has increased, additional fields have been modelled, such as those involved in a microphysics scheme, including various classes of liquid and ice phase mixing ratios, cloud fraction and the tendency terms defining the evolution of these fields. While the pri-

**Fig. 18** Radar observed rainfall rates at 1730 UTC 2 August 2002.

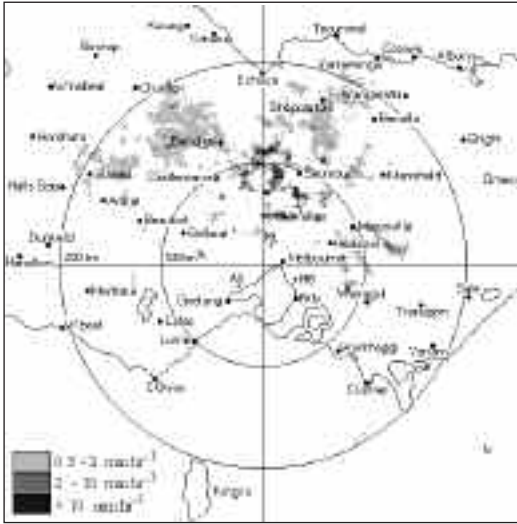


**Fig. 19** Radar observed rainfall rates at 1930 UTC 2 August 2002.

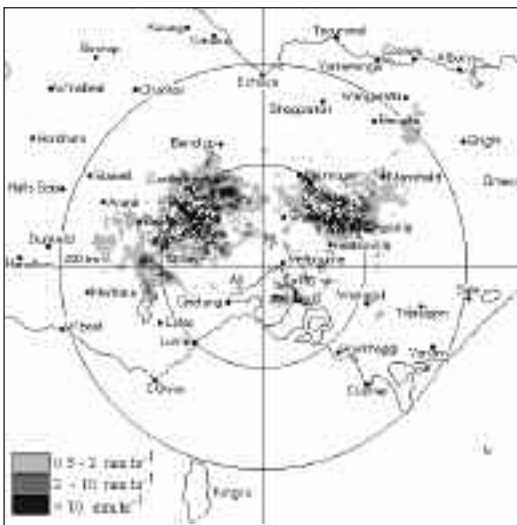
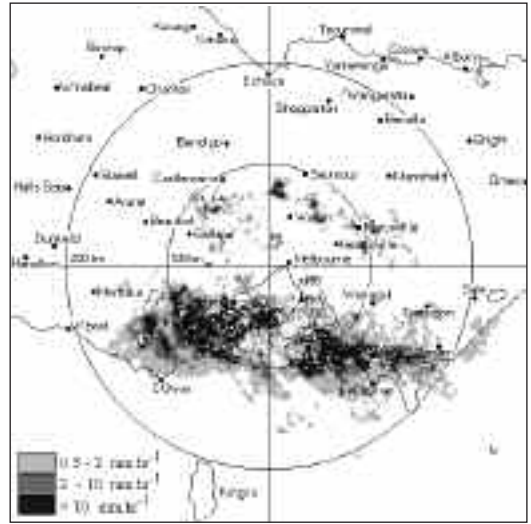


**Fig. 20** Radar observed rainfall rates at 2330 UTC 2 August 2002.



mary use of a microphysics scheme is to function as a component of a numerical model, there is an opportunity to analyse fields with the aim of extracting useful information that may otherwise be neglected.

A set of four indicators of convective activity has been developed based on information extracted from the bulk explicit microphysics scheme used in the LAPS model. Activation of these indicators depends on the explicit representation by the microphysics scheme of various features associated with convection. Essentially, the indicators are prognostic in nature as they rely on the ability of the numerical model to actu-

ally generate convective features within the model grid. Given a numerical model operating on a three-dimensional grid, the convective indicators are reduced to two-dimensional maps. This simple presentation of the indicators allows one to interpret the information rapidly, which is a requirement in an operational forecasting environment. While this representation minimises the amount of information required for interpretation, the analysis of the performance of the microphysics scheme at every model timestep, with eventual presentation of this information in the form of a percentage, ensures that simulations of short-lived weather systems are not overlooked.

Based on numerical simulations of two separate 24-hour periods, each containing observations of multiple precipitation features, the performances of the convective indicators have been tested. Overall, the four indicators performed well, providing useful and concise forecasts, while avoiding false identification of non-convective events. The indicators were able to identify various short-lived events occurring at different times within 24-hour periods. In general, indicators 1 (large rate of precipitation), 2 (hail potential) and 4 (lightning) produced forecasts of convection that were consistently in agreement with each other. While indicator number 3 (hydrometeor column) appeared to be slightly overactive (producing more false alarms than the other three fields), this may be avoided through adjustment of the thresholds. However, this behaviour is not wholly undesirable because it provides an approximate guide to the possibility of any development of con-

vective activity within the domain, in addition to that which may be predicted with more certainty by the other three indicators. It is expected that the convective indicators could be applied to virtually any microphysics scheme operating within a three-dimensional model grid. Suitable tuning of the thresholds would be required to adapt the convective indicators to individual models.

A prediction of some phenomenon at some location may, of course, be of great value to a forecaster, particularly when combined with other information. For example, numerical prediction of a thunderstorm may confirm the forecaster's belief of such development later in the day, or it may alert the forecaster to the possibility of such development over a particular region where it was otherwise not expected. This information may then allow a forecaster to review other relevant information before making a conclusion.

## Acknowledgments

Thanks to Drs N.E. Davidson, P.A. Riley, G.L. Roff and L.D. Rotstajn for reading the manuscript and providing constructive comments.

## References

- Atlas, D. and Williams, C.R. 2003. The anatomy of a continental tropical convective storm. *J. Atmos. Sci.*, *60*, 3-15.
- Bélair, S., Méthot, A., Mailhot, J., Bilodeau, B., Patoine, A., Pellerin, G. and Côté, J. 2000. Operational implementation of the Fritsch-Chappell convective scheme in the 24-hm Canadian regional model. *Weath. Forecasting*, *15*, 257-74.
- Bigg, E.K. 1953. The supercooling of water. *Proc. Phys. Soc.*, *B66*, 688-94.
- Byers, H.R. 1965. *Elements of cloud physics*. The University of Chicago Press, Chicago, 191 pp.
- Churchill, D.D. and Houze, R.A. Jr. 1984. Development and structure of winter monsoon cloud clusters on 10 December 1978. *J. Atmos. Sci.*, *41*, 933-60.
- Dare, R.A. 2004. The BMRC Bulk Explicit Microphysics Scheme. *BMRC Research Report No. 99*, Bur. Met., Australia.
- Gilmore, M.S. and Wicker, L.J. 2002. Influences of the local environment on supercell cloud-to-ground lightning, radar characteristics, and severe weather on 2 June 1995. *Mon. Weath. Rev.*, *130*, 2349-72.
- Hall, W.D. 1980. A detailed microphysical model within a two-dimensional dynamic framework: Model description and preliminary results. *J. Atmos. Sci.*, *37*, 2486-507.
- Hanstrum, B.N., Mills, G.A., Watson, A., Monteverdi, J.P. and Doswell, C.A.III 2002. The cool-season tornadoes of California and Southern Australia. *Weath. Forecasting*, *17*, 705-22.
- Hong, S.-Y., Juang, H.-M.H. and Zhao, Q. 1998. Implementation of prognostic cloud scheme for a regional spectral model. *Mon. Weath. Rev.*, *126*, 2621-39.
- Hsie, E.Y., Farley, R.D. and Orville, H.D. 1980. Numerical simulation of ice-phase convective cloud seeding. *Jnl appl. Met.*, *19*, 950-77.
- Johnson, R.H. and Hamilton, P.J. 1988. The relationship of surface pressure features to the precipitation and airflow structure of an intense midlatitude squall line. *Mon. Weath. Rev.*, *116*, 1444-72.
- Kessler, E. 1969. On the distribution and continuity of water substance in atmospheric circulations. *Met. Monogr.*, *10*, AMS, Boston, Mass., 84 pp.
- Kuo, Y.-H., Bresch, J.F., Cheng, M.-D., Kain, J., Parsons, D.B., Tao, W.-K. and Zhang, D.-L. 1997. Summary of a mini workshop on cumulus parameterization for mesoscale models. *Bull. Am. Met. Soc.*, *78*, 475-91.
- Lin, Y.L., Farley, R.D. and Orville, H.D. 1983. Bulk parameterization of the snow field in a cloud model. *Jnl Clim. Appl. Met.*, *22*, 1065-92.
- Lopez, P. 2002. Implementation and validation of a new prognostic large-scale cloud and precipitation scheme for climate and data-assimilation purposes. *Q. Jl R. Met. Soc.*, *128*, 229-57.
- Marshall, J.S. and Palmer, W.McK. 1948. The distribution of raindrops with size. *J. Met.*, *5*, 165-6.
- Mills, G.A. and Colquhoun, J.R. 1998. Objective prediction of severe thunderstorm environments: Preliminary results linking a decision tree with an operational regional NWP model. *Weath. Forecasting*, *13*, 1078-92.
- Molinari, J. and Dudek, M. 1992. Parameterization of convective precipitation in mesoscale numerical models: A critical review. *Mon. Weath. Rev.*, *120*, 326-44.
- Orville, H.D. and Kopp, F.J. 1977. Numerical simulation of the life history of a hailstorm. *J. Atmos. Sci.*, *34*, 1596-618.
- Puri, K., Dietachmayer, G.S., Mills, G.A., Davidson, N.E., Bowen, R.M. and Logan, L.W. 1998. The new BMRC Limited Area Prediction System, LAPS. *Aust. Met. Mag.*, *47*, 203-23.
- Rotstajn, L. 1997. A physically based scheme for the treatment of stratiform clouds and precipitation in large-scale models. I: Description and evaluation of the microphysical processes. *Q. Jl R. Met. Soc.*, *123*, 1227-82.
- Rutledge, S.A. and Hobbs, P.V. 1983. The mesoscale and microscale structure and organisation of clouds and precipitation in midlatitude cyclones. VIII: A model for the "Seeder-Feeder" process in warm-frontal rainbands. *J. Atmos. Sci.*, *40*, 1185-206.
- Saunders, C.P.R., Keith, W.D. and Mitzeva, R.P. 1991. The effect of liquid water on thunderstorm charging. *J. Geophys. Res.*, *96*, 11007-17.
- Schuur, T.J. and Rutledge, S.A. 2000a. Electrification of stratiform regions in mesoscale convective systems. Part I: An observational comparison of symmetric and asymmetric MCSs. *J. Atmos. Sci.*, *57*, 1961-82.
- Schuur, T.J. and Rutledge, S.A. 2000b. Electrification of stratiform regions in mesoscale convective systems. Part II: Two-dimensional numerical model simulations of a symmetric MCS. *J. Atmos. Sci.*, *57*, 1983-2006.
- Steiner, M. and Waldvogel, A. 1987. Peaks in raindrop size distributions. *J. Atmos. Sci.*, *44*, 3127-33.
- Sun, A., Chun, H.-Y., Baik, J.-J. and Yan, M. 2002. Influence of electrification on microphysical and dynamical processes in a numerically simulated thunderstorm. *Jnl Appl. Met.*, *41*, 1112-27.
- Tokay, A. and Short, D.A. 1996. Evidence from tropical raindrop spectra of the origin of rain from stratiform versus convective clouds. *Jnl Appl. Met.*, *35*, 355-71.
- Wilson, D.R. and Ballard, S.P. 1999. A microphysically based precipitation scheme for the UK Meteorological Office Unified Model. *Q. Jl R. Met. Soc.*, *125*, 1607-36.
- Wisner, C., Orville, H.D. and Myers, C. 1972. A numerical model of a hail-bearing cloud. *J. Atmos. Sci.*, *29*, 1160-81.
- Yuter, S.E. and Houze, R.A.Jr. 1997. Measurements of raindrop size distributions over the Pacific warm pool and implications for Z-R relations. *Jnl Appl. Met.*, *36*, 847-67.
- Ziegler, C.L., MacGorman, D.R. Dye, J.E. and Ray, P.S. 1991. A model evaluation of noninductive graupel-ice charging in the early electrification of a mountain thunderstorm. *J. geophys. Res.*, *96*, 12833-55.